Technical Report Documentation Page

1. Report No. SWUTC/10/476660-00070-1	2. Government Accession No.	3. Recipient's Catalog No.
4. Title and Subtitle Quantitative Characterization of Microstructure of Asphalt Mixtures		5. Report Date October 2010 6. Performing Organization Code
7. Author(s) Amit Bhasin, Swapneel Badgekar and Anoosha Izadi		8. Performing Organization Report No. Report 476660-00070-1
9. Performing Organization Name and Address Center for Transportation Research The University of Texas at Austin 1616 Guadalupe Street Austin, TX 78701		10. Work Unit No. (TRAIS) 11. Contract or Grant No. DTRT07-G-0006
12. Sponsoring Agency Name and Address Southwest Region University Transportation Center Texas Transportation Institute Texas A&M University System College Station, TX 77843-3135		13. Type of Report and Period Covered 14. Sponsoring Agency Code
15. Supplementary Notes Supported by a grant from the U.S. Department of Transportation, University Transportation Centers Program		

16. Abstract

The microstructure of the fine aggregate matrix has a significant influence on the mechanical properties and evolution of damage in an asphalt mixture. However, very little work has been done to define and quantitatively characterize the microstructure of the asphalt mastic within the asphalt mixture. The main objective of this study was to quantitatively characterize the three dimensional microstructure of the asphalt binder within the fine aggregate matrix of an asphalt mixture and compare the influence of binder content, coarse aggregate gradation, and fine aggregate gradation on this microstructure. Results indicate that gradation of the fine aggregate has the most influence of the degree of anisotropy whereas gradation of the coarse aggregate has the most influence on the direction anisotropy of the asphalt mastic within the fine aggregate matrix. Addition of asphalt binder or adjustments to the fine aggregate gradation also resulted in a more uniform distribution of the asphalt mastic within the fine aggregate matrix.

17. Key Words Asphalt Mixtures, Fatigue Cracking, Microstructure, X-Ray CT	18. Distribution Statement No restrictions. This document is available to the public through the National Technical Information Service, Springfield, Virginia 22161.		
19. Security Classif. (of report) Unclassified	20. Security Classif. (of this page) Unclassified	21. No. of pages 56	22. Price

Form DOT F 1700.7 (8-72) Reproduction of completed page authorized

QUANTITATIVE CHARACTERIZATION OF MICROSTRUCTURE OF ASPHALT MIXTURES

by

Amit Bhasin
Swapneel Badgekar
Anoosha Izadi

Research Report SWUTC/10/476660-00070-1

Southwest University Region Transportation Center
Center for Transportation Research
The University of Texas at Austin
Austin, Texas - 78712

October 2010

DISCLAIMER

The contents of this report reflect the views of the authors, who are responsible for the facts and the accuracy of the information presented herein. This document is disseminated under the sponsorhip of Department of Transportation, University Transportation Centers Program in the interest of information exchange. The U.S. Government assumes no liability for the contents or use thereof. This report is not intended for construction, bidding, or permits purposes.

ACKNOWLEDGMENTS

The authors recognize that support was provided by a grant from the U.S. Department of Transportation, University Transportation Centers Program to the Southwest Region University Transportation Center.

The authors would like to acknowledge the help of Mr. Christian Vasquez for his assistance with designing some of the mixtures used in this study and Dr. Jessie Maisano for her help with the X-ray CT scanning of the asphalt mixtures. The authors would also like to acknowledge Dr. Richard Ketcham from the Jackson School of Geosciences, The University of Texas at Austin, for his help with the Quant3D program and making modifications to the program that were required to accomplish the objectives of this study and Dr. Magdy Mikhail from Texas Department of Transportation for serving as a Project Monitor for this study.

ABSTRACT

The microstructure of the fine aggregate matrix has a significant influence on the mechanical properties and evolution of damage in an asphalt mixture. However, very little work has been done to define and quantitatively characterize the microstructure of the asphalt mastic within the asphalt mixture. The main objective of this study was to quantitatively characterize the three dimensional microstructure of the asphalt binder within the fine aggregate matrix of an asphalt mixture and compare the influence of binder content, coarse aggregate gradation, and fine aggregate gradation on this microstructure. Results indicate that gradation of the fine aggregate has the most influence of the degree of anisotropy whereas gradation of the coarse aggregate has the most influence on the direction anisotropy of the asphalt mastic within the fine aggregate matrix. Addition of asphalt binder or adjustments to the fine aggregate gradation also resulted in a more uniform distribution of the asphalt mastic within the fine aggregate matrix.

EXECUTIVE SUMMARY

Evidence in the literature suggests that the microstructure of the fine aggregate matrix has a significant influence on the mechanical properties and evolution of damage in an asphalt mixture. However, very little work has been done to define and quantitatively characterize the microstructure of asphalt mixtures. The first objective of this study was to identify quantitative metrics to characterize the microstructure of the fine aggreagte matrix within a full asphalt mixture. The second objective of this study was to use these metrics to compare the changes in the microstructure as a result of changes in binder content, gradation of coarse aggregates, and gradation of fine aggregates.

Based on a review of the literature, the star length distribution was identified as a means of defining the three dimensional geometry of the asphalt mastic that holds the fine aggregates together. X-ray computed tomography was used to obtain three dimensional images a selected volume from the full asphalt mixture. Two replicates of four different kinds of asphalt mixtures were used in this study. The star length distribution was used to compute the fabric tensor and determine the degree of anisotropy, orientation of the preferred direction of the asphalt mastic, average dimensions of the three dimensional asphalt mastic, and the variability of these dimensions.

Results indicate that gradation of the fine aggregate has the most influence of the degree of anisotropy whereas gradation of the coarse aggregate has the most influence on the direction anisotropy of the asphalt mastic. Addition of asphalt binder or adjustments to the fine aggregate gradation also resulted in a more uniform distribution of the asphalt mastic within the fine aggregate matrix. This could have a significant influence on mixture design and performance. For example, a matrix where the asphalt mastic has smaller average dimensions and is more uniformly dispersed can be more effective in crack pinning and hence resisting crack growth.

Another finding from this study is that, although all test specimens had gradations within the specification limits, they had widely different internal microstructures. The differences in the internal microstructure are expected to yield very different mechanical and damage characteristics. While the findings reported in this study are based on the use of a limited number of mixtures, the results highlight the importance of understanding the relationship between aggregate gradation, internal microstructure, and performance.

TABLE OF CONTENTS

LIST OF FIGURES

LIST OF TABLES

CHAPTER 1. INTRODUCTION

1.1 PROJECT BACKGROUND

Fatigue cracking is a significant form of pavement distress in flexible pavements. The most common method to quantify the resistance of asphalt mixtures to fatigue cracking and other distress mechanisms is to perform mechanical tests under controlled laboratory conditions on mixture specimens. The advantage of this approach is that candidate mixtures can be ranked based on their performance using a simple laboratory test. Another advantage of this approach is that it takes into account the combined affect of material and mixture properties on mixture performance. However, there are three major limitations to this approach. First, it does not provide any information that can be used to explain why certain mixtures perform better than others. This in turn limits the ability of the engineer to take cost effective remedial actions to improve the performance of poor performing mixtures. Second, the evolution of damage from some of the traditional laboratory performance tests is dependent on the test conditions (e.g. specimen geometry or mode of loading) and cannot be extrapolated to field conditions. Finally, the results obtained by conducting tests on full asphalt mixtures often have a very high variability. To alleviate some of these shortcomings, several research studies have been undertaken to investigate the properties and performance of asphalt mixtures at multiple length scales. For example, constituent materials (e.g. binder, aggregate, and fines) are evaluated in order to identify their contribution to mixture properties and damage evolution. Properties of mastics (fines mixed with asphalt binder) are evaluated to understand filler-binder interactions. Evaluation of sand-asphalt mortars or FAM provides information on the evolution of cracks, role of fines to arrest crack growth, and mechanisms of moisture damage. Evaluation of full asphalt mixtures helps identify the role of coarse aggregate properties and mixture microstructure in resistance of the mixture to damage.

There is significant evidence in the literature that demonstrates that the microstructure of the sand-asphalt dictates the mechanical properties and evolution of damage within the full asphalt mixture. However, in the context of asphalt mixtures the term microstructure is not well defined. There have been very few attempts to derive a quantitative metric for the microstructure of asphalt mixtures. Developing a quantitative method to describe the three dimensional microstructure of asphalt mixtures has several potential applications and advantages. For example, a quantitative measure of the microstructure of asphalt mixtures can be used to (i) characterize the average three dimensional geometry of the matrix that holds the aggregates together (where matrix may refer to the binder, mastic, or mortar depending on the length scale of interest), (ii) estimate the level of anisotropy of different components within the asphalt mixtures, (iii) understand the relationship between geometry of the matrix and performance related aspects such as development of confining

stresses, and (iv) estimate the influence of aggregate shape, gradation, and binder content on the shape of the matrix.

1.2 OBJECTIVES OF THIS STUDY

The main objective of this study is to address the first and most critical step in the pursuit of relating mixture microstructure to its properties, i.e. to establish a quantitative method to characterize the three dimensional microstructure of the asphalt binder and filler matrix or mastic in an asphalt mixture. This was achieved by accomplishing the following key steps.

- Asphalt mixture specimens with different aggregate gradations and binder contents were fabricated in the laboratory.
- Representative volumes of these asphalt specimens where then scanned using very high resolution three-dimensional X-ray computed tomography (X-Ray CT). Note that unlike previous studies, the focus of this study was to evaluate the three dimensional microstructure of asphalt binder or mastic in a mixture. Consequently, smaller representative portions of the full asphalt mixture specimen were scanned using very high resolution X-ray CT instead of lower resolution scans of full asphalt mixture specimens.
- The scanned gray scale X-ray CT images were processed to eliminate noise and determine the gray scale thresholds that separate the three phases, asphalt binder, aggregate and air voids based on measured volumetric properties.
- The star length distribution (SLD) parameter was used to characterize the shape of the asphalt binder matrix in the mixture. Change in aggregate gradation and binder content was used to describe the change in microstructure of the asphalt mixtures via the SLD parameter.
- Parameters based on the SLD such as the fabric tensor were used to estimate the level of anisotropy in the mixture. Variability in the SLD was used to quantify the expected variability in the mixture properties along specific directions.

1.3 REPORT STRUCTURE

This report consists of five chapters. The first chapter in on the project background and objectives of this study. The second chapter summarizes the findings from a detailed literature review on three aspects, (i) importance of internal microstructure on the performance of asphalt mixtures and methods used to determine the internal microstructure, (ii) methods to pre-process and enhance images, and (iii) metrics to quantify internal microstructure of composite materials and relationship of these metrics to mechanical properties of the composite. The third chapter presents details of

the methodology used to fabricate specimens, collect and process the image data. Chapter four presents the detailed analysis of results and chapter five presents a discussion of findings and conclusions from this study.

CHAPTER 2. BACKGROUND AND LITERATURE REVIEW

2.1 INTERNAL STRUCTURE OF ASPHALT MIXTURES AND OTHER COMPOSITES

The term internal structure of an asphalt concrete mixture refers to the content and spatial distribution of asphalt, aggregates and air-voids (Masad et al., 1999a). The internal structure of the mixture is dictated by the proportions and properties of its constituent materials and method of compaction. It is well recognized that the internal structure of an asphalt mixture plays a significant role in influencing the mechanical properties and the resistance of the mixture to major distresses including rutting, fatigue cracking, thermal cracking and low temperature cracking. Most mixture design methods recognize the importance of internal microstructure by imposing requirements for aggregate size, gradation, shape, limits on density during compaction, and volumetrics (Masad and Button, 2004). In the past decade several research studies have used more direct methods, such as imaging techniques, to characterize the internal microstructure of asphalt mixtures. Three basic steps are typically required the characterize the internal microstructure using this direct approach. The first step is to acquire two-dimensional (2D) or three-dimensional images (3D) of the composite. Digital cameras can be used to acquire 2D image of a cross-section or a series of images for cross-sections that are obtained by physically dissecting the specimen into several slices. An alternative approach is to use non-destructive techniques such as 3D X-ray tomography that provide a stack of 2D images for a volume of interest at varying resolutions. The second step is to process the image to eliminate noise and identify regions of interest (e.g. aggregate, air void). Section 2.2 presents more details on image processing. The last step is to identify metrics that can be used to quantify the characteristic of interest (e.g. size of voids, orientation of aggregates). Section 2.3 presents more details on image analysis.

Image analysis of internal microstructure has been applied in three broad areas discussed below. First, image analysis has been used to investigate the influence of compaction on the internal microstructure of asphalt mixtures. For example, Masad et al. (1999a) used X-ray tomography to establish the relationship of aggregate orientation, aggregate gradation, and air void distribution to the compaction effort. The study included specimens compacted in the laboratory using the Superpave gyratory compactor (SGC) with different number of gyrations as well as field cores. The orientation of an aggregate was measured as the angle between its major axis and a horizontal line on the scanned image. Anisotropy in aggregate orientation was quantified based on the distribution of the aggregate orientations. Aggregate and air void size distributions were obtained by measuring the area on the two-dimensional sectional images obtained from X-ray tomography. The bias due to the use of two-dimensional sectional images to obtain aggregate size distribution was corrected using Monte-Carlo simulations. Due to limitations in the resolution of images obtained from the

X-ray tomography, comparison of aggregate size distribution and orientation to the compaction effort was limited to coarse aggregates. Masad et al. (1999a) concluded that specimens compacted using a low number of gyrations resulted in a uniform void distribution throughout the specimen height. On the other hand, at higher number of gyrations the middle part of the specimen had fewer air voids. In another study, Masad et al. (1999b) quantified the internal structure of the asphalt mixtures in terms of the aggregate orientation, points of contact and distribution of air voids. These characteristics were compared for mixtures compacted using the SGC and the linear kneading compactor (LKC). The erosion operation technique was used to determine the number of contact points. Masad et al. (1999b) concluded that the aggregates in the SGC have preferred orientation toward horizontal direction while aggregates in the LKC had a more random distribution. They also concluded that the aggregates in LKC specimens had more point to point contacts as compared to the SGC specimens. They suggested that higher aggregate contact points in the LKC specimens resulted in higher shear strength in specimens compacted using the LKC due to inter particle contact. Finally, they concluded that air voids were concentrated at the top and the bottom portions of the SGC compacted specimens and at the bottom of the LKC specimens. Hunter et al. (2004) also investigated the change in internal microstructure of asphalt mixtures as influenced by the method of compaction. Radial and circumferential particle alignment and area of particles in fixed radial quadrants were used to examine variations in aggregate orientation and distribution within the asphalt mixture. They concluded that depending on the method of compaction, mixtures with similar bulk volumetric properties demonstrated different levels of preferred circumferential and radial orientations.

Second, image analysis has been used to investigate the influence of internal microstructure on the engineering properties and performance of asphalt mixtures. For example, Yue et al. (1995) used image analysis to quantify anisotropy in an asphalt mixture based on the orientation of aggregates. Directional distribution of aggregates was quantified based on the ratio of average area per aggregate in horizontal sections to the average area per aggregate in vertical sections. Wang et al. (2001) demonstrated that field cores with similar volumetric properties exhibited different internal microstructure that correlated better with their observed field performance. Void content, void distribution, and mean solid path were measured on sectional images obtained using X-ray tomography. An interpolation algorithm was developed and used to create intermediate sectional images in order to compensate for the lower vertical resolution as compared to the horizontal resolution for the images. Masad et al. (2002) and Tashman et al. (2005) used two dimensional image analysis to quantify aggregate distribution on cut sections of asphalt mixtures to determine the level of anisotropy. They then used this as one of the model parameters to improve the predictions of viscoplastic deformation in asphalt concrete mixtures. Arambula et al. (2007) demonstrate that the aggregate gradation and compaction effort influence the size and distribution of air voids within an

asphalt mixture. The size and distribution of air voids were shown to have a strong influence on the rate of moisture damage in the asphalt mixtures.

The relationship of internal microstructure and mechanical properties has also been long recognized for materials other than asphalt mixtures. For example, according to Ryan and Ketcham (2002) the relationship between the trabecular bone morphology and skeletal loads was first investigated in 1867. Cowin (1985) investigated the relationship between the stiffness tensor of a trabecular bone to its "fabric". He introduced the term fabric as a measure of the local anisotropy of a material's microstructure. Duxson et al. (2005) demonstrated a correlation between mechanical strength and Young's modulus of geopolymers and their microstructure .

Finally, image analysis has been used to derive the internal microstructure of asphalt mixtures that serves as the required geometry input for computational modeling. For example, Wang et al. (2007) describe methods to extract three dimensional geometric features of aggregates from X-ray CT images. Zhanping et al. (2009) developed a two dimensional and three dimensional discrete element model to predict the dynamic modulus of asphalt concrete mixtures. The required geometry for these models was obtained using X-ray CT imaging. The authors reduced the three dimensional images of real asphalt mixtures into three different components, coarse aggregates, fine aggregate-binder mortar, and air voids. Zelelew et al. (2008) developed volumetric based global minima thresholding algorithm to process asphalt concrete X-ray CT images. This technique was used to distinguish between air, mortar and coarse aggregates within a full asphalt mixture based on the volumetric properties of the mixture thus allowing for a more accurate and calibrated geometric representation of these components that can be used in subsequent computational modeling. Tutumluer et al. (2008) used imaging methods to extract the geometry of aggregates used in granular materials for discrete element modeling (DEM). They used DEM to demonstrate the influence of aggregate angularity and surface texture on the shear properties of granular base materials.

The previous studies have recognized the importance of the distribution or structure of the internal structure of asphalt mixtures. However, most of this work focused on the characterization of aggregate size, distribution and orientation of the distribution of air voids. Very little work has been done to quantitatively characterize the microstructure of the matrix, i.e. asphalt binder or mastic that holds the mixture together. In 1930s Hveem introduced the concept of film thickness to design asphalt mixtures. The methods used to calculate the film thickness (that would result in optimal performance of the mixture) were approximate and relied on several unrealistic assumptions. More recently, Elseifi et al. (2008) used reflective light microscopy and scanning electron microscopy to demonstrate that a uniform film coating the aggregates did not actually exist in the asphalt mix. They demonstrated that film thickness varied greatly within the same specimen and around the same aggregate. They also reported that mineral fillers and finer aggregates were embedded in the asphalt binder such that the behavior of the binder itself may not be as critical as the behavior of

the mastic. The focus of this study is placed on identifying quantitative metrics to characterize the microstructure of the asphalt or mastic matrix in the composite.

In summary, distribution of air voids, solid path between air voids, orientation and points of contacts between coarse aggregates were typically used as the metrics to describe the internal microstructure of asphalt mixtures. In most cases, these metrics were obtained using individual 2D sectional images of a mixture specimen and do not directly characterize the binder matrix. The objective of this research was to identify a method and concomitant parameter by which to quantify the three dimensional internal microstructure of asphalt binder or mastic based on the collective analysis of all sectional planes for a mixture specimen obtained using x-ray tomography. Although the methodology discussed in this report is applied to characterize the internal microstructure of the asphalt mastic, it can also be used to characterize the three-dimensional microstructure of any component in the mixture (e.g. air voids, aggregates, mortar).

2.2 IMAGE PROCESSING

Digital images acquired from X-ray CT scanning or any other method are typically in gray scale and contain some amount of noise. The acquired images must be processed prior to use for any kind of analysis. This section presents a short review of some of the methods that were investigated and used to process the images used in this study. Image processing can be broken down into three major steps:

1. Contrast enhancement
2. Noise reduction
3. Thresholding

Each one of these key steps are briefly discussed in the subsections below.

2.2.1 Contrast Enhancement

Although contrast enhancement is not critical for computational analysis of images, it is usually performed to improve visibility of image and allows the user to clearly differentiate the components in an image. There are two techniques available to perform contrast enhancement,

- histogram equalization and
- best fit equalization.

Histogram equalization is the most common technique used for contrast enhancement. Histogram equalization is achieved by transforming a small range of values from an intensity image (or the

values in the color map of an indexed image), so that the histogram of the output image approximately matches a specified histogram with a broader range of values. For example, Figure 2.1 shows application of histogram equalization technique on an image of an asphalt concrete mixture. The original image in Figure 2.1 has intensity values ranging from 0-165, while the image after histogram equalization spans full range of available intensity values, i.e. 0-256. The best fit equalization method maps the intensity values from the original gray scale image to new values such that 1% (can be varied) of data is saturated at low and high intensities of the original image. This increases the contrast of the output image. Figure 2.2 illustrates the typical results from using the best fit equalization on an image of an asphalt concrete mixture.

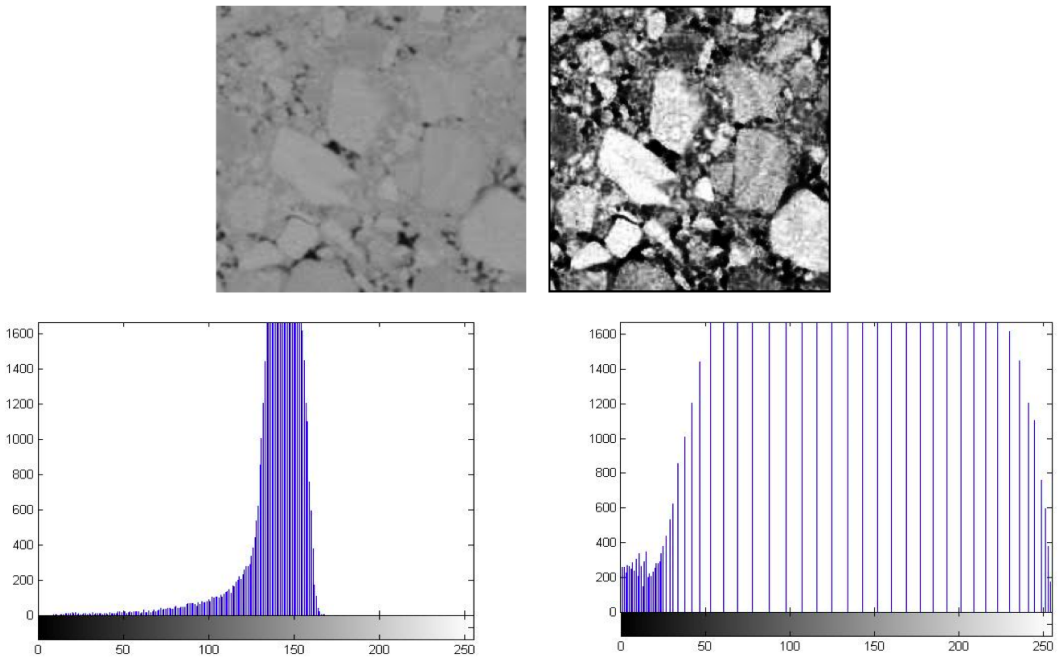

Figure 2.1. Contrast Enhancement Using Histogram Equalization.

(Left: Before Enhancement, Right: After Enhancement)

2.2.2 Noise Reduction

This is perhaps the most important step in image processing. Noise is defined as random, usually unwanted, variation in brightness or color information of an image. This randomness leads to erroneous interpretation of image data and hence needs to be addressed before any analysis is carried out. In the case of X-ray CT images, the most common source of noise is counting statistics in the image detector due to a small number of incident particles such as electron or photon (Russ, 2007). Other common sources include inadequate or non-uniform illumination, undesirable viewpoint, issues with alignment, sensor quality, as well as image digitizing and pre-processing.

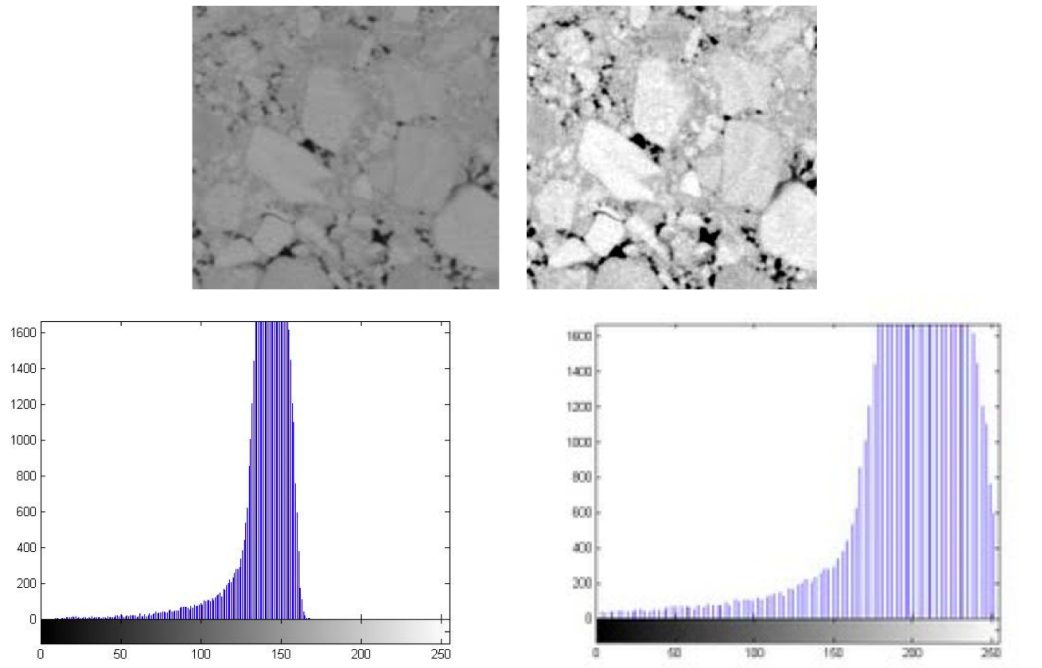

Figure 2.2. Contrast Enhancement Using Best Fit Equalization.

(Left: Before Enhancement, Right: After Enhancement)

In general, the common types of noise associated with images are random (or Gaussian) noise, shot (or salt pepper) noise, film grain, and non-isotropic noise. Random noise is the most common form of noise in images of asphalt concrete mixtures obtained using X-ray CT images. Images from X-ray CT scanning can also have artifacts due to beam hardening, a process by which X-rays with lower intensity are attenuated while rays with higher intensity continue to traverse through the medium.

There are three common methods that can be used to reduce random noise. There are several different sub-methods under for each one of these three methods:

- neighborhood averaging,
- median neighborhood ranking, and
- mode neighborhood ranking.

The underlying assumption to apply these methods is that pixels in the image are much smaller than any of the important details. Another assumption is that the structure represented by a pixel and its neighborhood is very similar. The basic principle for the three methods is the same, i.e. for a given pixel, its original intensity value is replaced by a new value obtained by performing a mathematical operation on the intensity values of the neighboring pixels. In case of the neighborhood

averaging method, the intensity of a pixel is replaced by the mean intensity of the pixels within a defined neighborhood of the subject pixel. Similarly, in the case of median or mode ranking methods, the pixel intensity is replaced by the median or mode of intensity of pixels within a defined neighborhood of the subject pixel. An important variable in applying these techniques is the size of the neighborhood that is used to compute the intensity of a pixel based on its mean, median or mode.

As stated above, neighborhood averaging replaces the original value of a pixel with the average of pixel values around its neighborhood. The advantage of this technique is that it is very effective in reducing shot noise. However, one limitation of this method is that it blurs the edges of different entities within the image. This in turn reduces the accuracy of edge detection that may be performed on the images later. Neighborhood averaging also results in boundary displacement and contrast reduction. Other variations of neighborhood averaging such as weighted average filter, and Olympic filter may be used to offset these limitations to some extent. Figure 2.3 presents an original and filtered image by performing neighborhood averaging using a 3x3 matrix and a 9x9 matrix. Notice that the use of a larger matrix size (averaging across a larger neighborhood) results in reduced noise but greater distortion in the image.

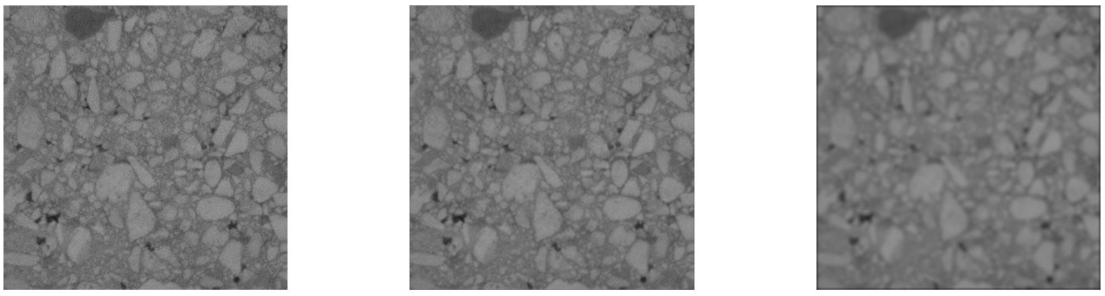

Figure 2.3. Use of Neighborhood Averaging to Reduce Noise.

(Left: Before Filtering, Middle: Neighborhood Averaging with 3x3 Matrix, Right: Neighborhood Averaging with 9x9 Matrix)

In the median neighborhood ranking method, the pixel value is replaced by median of neighborhood pixel values. This involves ranking of pixel intensity values within a neighborhood and assigning the median value to the central pixel. This technique overcomes most of the limitations of neighborhood averaging, especially related to blurring of edges. Also, as the name suggests, median neighborhood ranking is not as sensitive to outliers or extreme data points in the neighborhood as compared to the neighborhood averaging. It is useful in reducing shot noise and it does not result in shifting of boundaries or reduced brightness difference across steps. The main limitation of this technique is that it erases fine lines and rounds corners. However, if the objective of image

analysis is to detect features and separate different entities within the image, as in the case of analysis of the internal structure of asphalt mixtures, the median neighborhood ranking method would be preferred to the neighborhood averaging method. Figure 2.4 presents an original and filtered image by performing median neighborhood ranking.

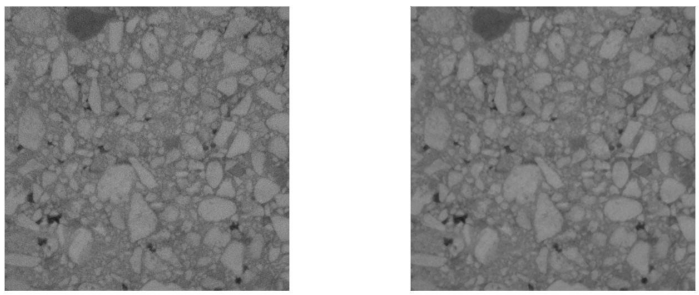

Figure 2.4. Use of Median Neighborhood Ranking with 3x3 Matrix to Reduce Noise.

(Left: Before Filtering, Right: Median Neighborhood Ranking)

The mode neighborhood ranking filter replaces the value of each pixel with the mode of the pixel values in its neighborhood. Although this filter has many advantages over the previous two filters, a serious limitation is that it can be used with a small neighborhood. Therefore, this technique was not considered appropriate for this study.

2.2.3 Thresholding

An asphalt mixture is made up of three components, air, asphalt binder (or mastic = binder + fines), and aggregates. Each of these components has a significantly different density from the other. In order to characterize the internal structure of the asphalt mixture it is of interest to clearly differentiate these three components in the image. X-ray CT images of asphalt mixture specimens are created by measuring the attenuation of the X-rays traveling through the specimen. The amount of attenuation is proportional to the density of the material. Consequently, a high intensity or bright pixel indicates a high density material (such as an aggregate) and a dark pixel indicates a low density material or phase (such as air void). However, due to inherent variability in the densities of these materials and finite resolution of the imaging process, the X-ray CT images do not contain three pixel intensity values corresponding to each of the three components. Instead, the CT images are gray scale images with pixel values ranging from 0 to 255. Thresholding is the most critical step that allows the user to reduce these gray scale images to binary or trinary images with just two or three pixel values to represent any two or three components of interest. The following is a brief review and background of approaches for thresholding a gray scale image to a binary image that clearly distinguishes between the two components of a composite using two different pixel

intensity values. The same concepts can be extend to obtain a trinary image that uses three pixel intensity values to represent three components in the composite.

Thresholding can be performed either automatically based on standard algorithms or manually based on specific algorithms defined by the user. The automatic approach works on the principle that there are only two components present in the image and the threshold level is defined as the pixel value that separates these two components. Figure 2.5 shows histogram for such a composite. For this example, a typical automated thresholding algorithm will tend to select the pixel value that produces the smallest value between the two peaks. For Figure 2.5 this threshold level value is approximately 125. Figure 2.6 illustrates the results from applying the automatic threshold algorithm to a typical image of an asphalt concrete specimen. The threshold level selected by program to differentiate aggregates from air, asphalt binder and possibly fine aggregates, was 129.5. The main advantage of this method is that the results are consistent and no judgment is involved in the approach. However, this automated approach can only be applied when there are only two easily distinguishable components present in the image. There are several instances, in which such an automated algorithm can very easily produce misleading results.

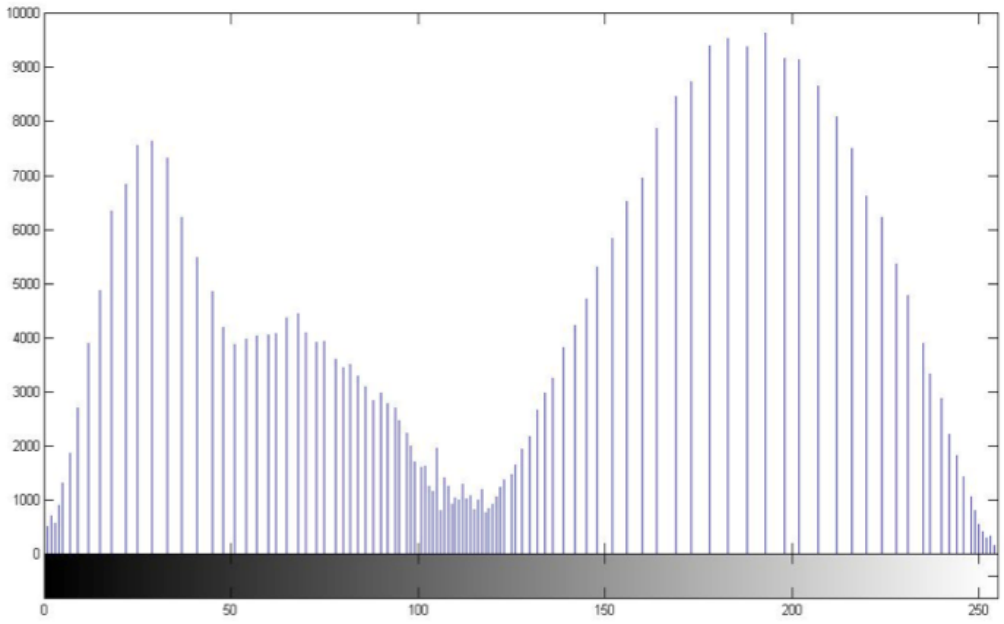

Figure 2.5. Histogram of a Composite With Two Components.

There are two ways to mitigate the limitations associated with the automatic approach. The first is to manually select a threshold based on the users judgment. This approach can be highly subjective and result in inconsistent interpretation of results from image analysis depending on the

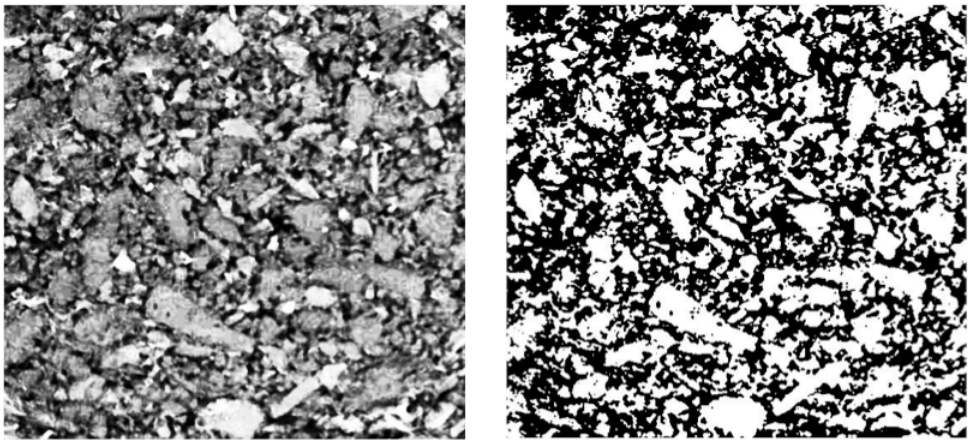

Figure 2.6. Thresholding of a Gray scale Image to Binary Image Using Automated Algorithm.

user. Figure 2.7 shows the results from application of manual thresholding on the same image as in Figure 2.6 with threshold level 73 to differentiate aggregates from air, asphalt binder and possibly fines. The second and more robust approach is to iteratively select different thresholds until the measured area fraction (or volume fraction) of each of the two components from the image (or a stack of images representing a three dimensional structure) matches previously known or directly measured area fraction (or volume fraction). Section 2.2 of this report presents more details on this approach that was also used in this research.

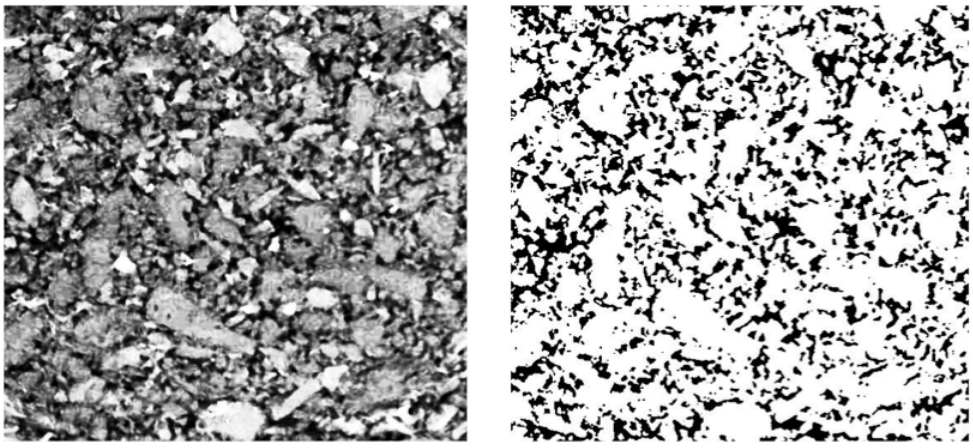

Figure 2.7. Manual Thresholding of a Gray scale Image to a Binary Image.

2.3 IMAGE ANALYSIS

The previous section presented different methods to process raw digital images with the objective of reducing noise and converting a gray scale image to a binary or trinary image that reflect the two or three different components of interest in an asphalt mixture. The next step is to use these images to draw out meaningful information regarding the microstructure of the components within the mix. This section, presents a review of the various metrics and methods that can be used to characterize the internal structure of a composite using three dimensional X-ray CT images. Section 2.1 introduced some of these metrics that have been used for asphalt mixtures. For example Masad et al. (1999b) quantified aggregate anisotropy using the angle of the major axis of the aggregate to the horizontal axis of the image. The focus of this section will be to review techniques that can be used to quantify the shape characteristics of the matrix (asphalt binder or mastic) in the composite.

Image analysis of a composite generates a variety of measurements on the individual material objects within the composite including volume, orientation, shape, and surface area. A continuous quantity that varies with orientation can be used to quantify the orientation and distribution of material objects within the composite. Examples of such quantities that have typically been used in the literature are mean intercept length (MIL), chord length, star length, and star volume.

One of the simplest direction dependent quantities that can be used to characterize the microstructure of a two component composite is the mean intercept length (MIL) (Harrigan and Mann, 1984). The MIL along a direction is obtained as follows: grid lines are drawn at specific intervals along the direction on an image of the two-component composite. The intersections between the grid lines and the interface of the two-components are counted. The mean intercept length is then defined as the total length L of the line grid divided by the number of intersections (Figure 2.8). The MIL can be obtained along several different directions. A drawback of the MIL is that it determines the orientation of the interface rather than the material itself and it may underestimate the anisotropy of the material. An alternative and similar approach is the chord length density distribution. The chord length distribution along a direction is obtained as follows: similar to the MIL grid lines are drawn on an image of the two-component composite and lengths of chords between the intersections of grid lines are measured (Figure 2.8). The chord length distribution (CLD) function $p(z)$ indicates that the probability of finding a chord of length between z and $z+dz$ is $p(z)\,dz$ (Torquoato and Lu, 1993).

Two additional direction dependent quantities are the Star Length Distribution (SLD) and Star Volume Distribution (SVD) (Odgaard, 1997). The star length distribution is calculated by randomly selecting several points in the material of interest within the composite and measuring the length of lines emanating from these points in various directions until the lines encounter a bound-

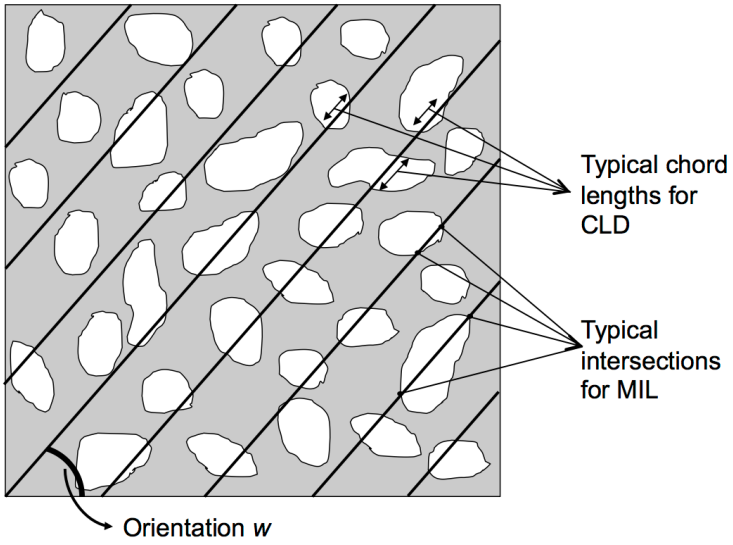

Figure 2.8. Schematic of MIL and CLD Measurements in a Two Component Composite.

ary. By doing so, the distribution of the material of interest is obtained. The orientations along which the lines emanate from the points are typically predefined by selecting a homogeneous distribution of points on a unit sphere. Increasing the number of points reduces the uncertainty and is more efficient than increasing the number of orientations. The average star length along an given orientation is computed as:

$$S_w = \frac{1}{n}\sum_{i=1}^{n} L_i \tag{2.1}$$

where, L is the length of measured intercept through point i at orientation w and n is the number of points. The SLD can be obtained for any single material that is of interest within a multi-component composite. Figure 2.9 illustrates the measurement of SLD at four points in two dimensions (in practice the measurements are carried out in three dimensions). The star volume distribution (SVD) is similar to SLD with the only difference that instead of instead a straight line along a particular direction, the volume of a cone emanating from a point in a predefined orientation is measured. The average star volume along any given orientation is computed as:

$$U_w = \frac{\pi}{3n}\sum_{i=1}^{n} L_i^3 \tag{2.2}$$

where, L and n are as described before. The difference between SVD and SLD is that SVD tends to amplify the differences between major and minor components, enhancing the effect of anisotropy. For a more detailed description of these two methods, the readers are referred to Odgaard (1997).

The aforementioned parameters (MIL, CLD, SLD, and SVD) provide the distribution and mean

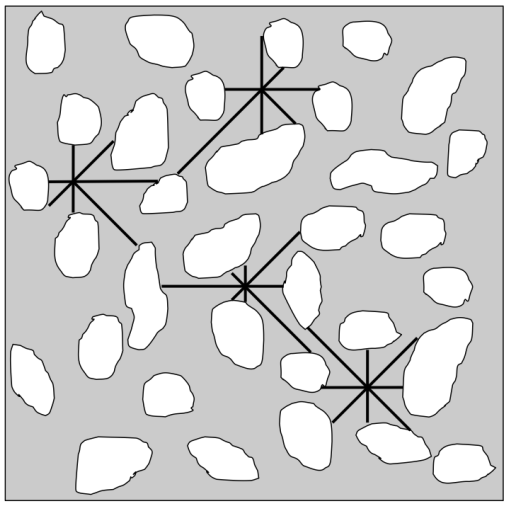

Figure 2.9. Schematic of SLD Measurements at Four Points in a Two Component Composite.

of a characteristic quantity along different orientations in a composite. A 2D or 3D rose diagram of the mean of any one of these characteristics along different orientations provides an excellent visual representation of the internal microstructure. However, it is also important to use this information to quantitatively derive parameters that relate to the mechanical properties of the composite. One such parameter, that will be used later to characterize the microstructure of the asphalt mastic, is the fabric tensor based on the moment of inertia. Consider that the star lengths are measured at n points along w orientations to produce a data set of N vectors represented by $\mathbf{a}_i$, where $i = 1$ to N.

$$\mathbf{a}_i = \begin{bmatrix} a_{xi} \\ a_{yi} \\ a_{zi} \end{bmatrix} \tag{2.3}$$

Watson (1966) proposed that the orientation matrix or fabric tensor for this data set is mathematically obtained as follows.

$$\mathbf{T} = \sum_{i=1}^{N} \mathbf{a}_i \mathbf{a}_i^T = \begin{bmatrix} \sum_{i=1}^{N} a_{xi}^2 & \sum_{i=1}^{N} a_{xi}a_{yi} & \sum_{i=1}^{N} a_{xi}a_{zi} \\ \sum_{i=1}^{N} a_{xi}a_{yi} & \sum_{i=1}^{N} a_{yi}^2 & \sum_{i=1}^{N} a_{yi}a_{zi} \\ \sum_{i=1}^{N} a_{xi}a_{zi} & \sum_{i=1}^{N} a_{yi}a_{zi} & \sum_{i=1}^{N} a_{zi}^2 \end{bmatrix} \tag{2.4}$$

The orientation matrix or fabric tensor $\mathbf{T}$ has three eigenvalues $\hat{\tau}_1 > \hat{\tau}_2 > \hat{\tau}_3$ and corresponding eigen vectors $\hat{\mathbf{u}}_1$, $\hat{\mathbf{u}}_2$, $\hat{\mathbf{u}}_3$ (Watson, 1966; Ketcham, 2005b). For any axis represented by vector $\mathbf{u}$,

the moment of inertia $I(\mathbf{u})$ is given by equation 2.5.

$$I(\mathbf{u}) = \sum_{i=i}^{N} |a_i|^2 - \mathbf{u}^T \mathbf{T} \mathbf{u} \tag{2.5}$$

Finally, the eigen vectors $\hat{\mathbf{u}}_1$ and $\hat{\mathbf{u}}_3$ also represent the direction vectors along which the moment of inertia is minimized and maximized, respectively. The eigen vectors can be used to derive important parameters that reflect the properties of the composite. For example, the degree of anisotropy can be computed as $\hat{\tau}_1/\hat{\tau}_3$ and elongation index as $1-(\hat{\tau}_2/\hat{\tau}_1)$ (Ketcham, 2005b). Based on this review, for this research metrics based on the SLD, i.e. the fabric tensor and the degree of anisotropy were used to compare the microstructure of different asphalt mixtures.

CHAPTER 3. MATERIALS, DATA COLLECTION AND PROCESSING

The previous chapter presented a summary from a literature review on the importance of internal structure of asphalt mixtures. The previous chapter also presented a review of the different methods to process images prior to analysis as well as image analysis tools and metrics that can be used to characterize the internal structure of asphalt mixtures. This chapter presents the research methodology adopted to achieve the objective of this project, i.e. to characterize the internal microstructure of the matrix that holds the aggregates together in an asphalt mixture, i.e. the asphalt binder or mastic.

The preliminary research and literature review identified three milestones to perform this study – data collection, image processing and image analysis. The data required for this study was in the form of images representing internal structure of asphalt specimens. The data collection task was divided into two activities, preparing asphalt specimens of desired gradation in laboratory and scanning the above specimens and obtaining images. The following sections of this chapter present more details on the materials and methods used to fabricate test specimens and imaging of the specimens using the micro X-ray CT scanner. The images obtained after scanning of specimens were processed to meet certain requirements and then analyzed with the statistical tools to describe the microstructure of the asphalt binder mastic in the mixture. Figure 3.1 illustrates the flowchart of activities performed to achieve the objectives of this research. Chapter 4 of this report presents more details on the methods used for image processing and analysis followed by Chapter 5 that presents a discussion of findings from this research study.

3.1 SELECTION OF MATERIALS AND SPECIMEN FABRICATION

The primary objective of this study was to identify metrics that can be used to quantify the shape characteristics and variability in the microstructure of asphalt or mastic matrix in an asphalt mixture. To achieve the objective of this study, a typical dense graded asphalt mixture was selected. Three additional variations of this mixture were produced in the laboratory by changing the binder content, coarse aggregate gradation, and fine aggregate gradation to produce a total of four different mixtures. The four mix designs were labelled as *control*, *high binder*, *coarse adjusted*, and *fine adjusted*. The aggregate used in all mixtures was a limestone obtained from RTI South Plant, Buda, Texas. Limestone is well suited for X-ray CT scanning because of its relatively homogeneous mineral makeup compared to other aggregates. Although igneous aggregates or gravels may also be used, these aggregates typically contain minerals with varying densities that may result in non-uniform X-ray attenuation and artifacts in the CT images. The asphalt binder had a performance grade of PG 64-22.

Figure 3.2 shows the gradation and binder content for these four mixtures. The gradation limits are based on the specification followed by the Texas Department of Transportation (TxDOT) for Type C mixtures and all variations of the control mix were designed to be within these limits. The *control mix* had 4.2% binder content by weight of aggregates, and the *high binder* mix had 4.7% binder content but the same aggregate gradation as the control mix. The coarse adjusted mix had the same binder content and fine aggregate (passing #16 sieve) gradation as the control mix but the gradation of the coarser aggregates (retained on #16 sieve) was modified. Similarly, the fine adjusted mix had the same binder content and coarse aggregate gradation as the control mix but the fine aggregate gradation was modified.

It is important to emphasize that all four mixes used the same binder and aggregate and only difference between the control and other mixes was either the binder content or the gradation. The rationale for selecting these four mixtures was not to establish a correlation between the micro structure of the mastic and mixture characteristics (although this is the eventual long term goal). Rather, these four mixtures were selected to (i) evaluate the influence of these parameters on the micro structure of asphalt mixtures, and (ii) to evaluate whether or not the metrics used to quantify the mastic micro structure are sensitive to changes in mixture characteristics.

The maximum specimen size that can be used with the three dimensional X-ray CT scanner is dictated by the resolution required for micro structure characterization. The objective of this study was to characterize the internal micro structure of binder or mastic matrix in an asphalt mixture. Accordingly, a resolution in the range of 10 micrometers per voxel was considered as appropriate for this study. A cylindrical specimen approximately 12.5 mm in diameter was considered as appropriate to achieve this resolution. Asphalt mixture specimens that were six inches in diameter and four inches in height were compacted for each of the four different mixtures using the Superpave gyratory compactor (SGC). The ends of the SGC compacted specimen were cut using a diamond blade saw to achieve a finished specimen height of two inches. A diamond coring bit was used to core approximately ten specimens that were 12.5 mm in diameter and 50 mm in height. Two specimens cored from the SGC compacted specimen for each type of mixture were selected for X-ray CT scanning. The two cored specimen were selected such that they had similar air void content as compared to the average air void content of the SGC compacted specimen.

3.2 HIGH RESOLUTION X-RAY CT SCANNING OF IMAGES

The finished specimens were used to obtain high resolution sectional images of the test specimen from a volume of interest. The scanning was performed at the high-resolution X-ray CT Facility at the University of Texas at Austin (UTCT). Ketcham and Carlson (2001) provide a more detailed description of the principles of X-ray tomography and methods used to acquire images and correct artifacts. In summary, high-resolution X-ray CT scanning (HRXCT) is based on the principle that

an X-ray fan beam (or cone beam) is directed at an object from all orientations in a plane, and the decrease in X-ray intensity caused by passage through the object is measured by a linear array of detectors (Figure 3.3). The resulting data are then reconstructed to create a cross-sectional image of the object along that plane. The gray scales in such images reflect the relative linear X-ray attenuation coefficient μ, which is a function of density, atomic number, and X-ray energy. For this study, the energy source used was adjusted to 80kV and 10W to obtain the best resolutions.

Each CT image is termed a 'slice', as it corresponds to what one would see if the object were sliced along the scan plane. By gathering a stack of contiguous slices, data for a complete 3D volume can be obtained. Each slice represents a finite thickness of material, corresponding to the thickness of the collimated X-ray beam and detector array. Consequently, the pixels in CT images represent volume elements and are referred to as voxels Ketcham (2005a).

A total of 8 specimens, two of each mixture type, were scanned using the HRXCT. A volume, approximately 12.5 mm x 12.5 mm x 8 mm, enclosing the middle third of each specimen was scanned to obtain a total of 562 images each with a resolution of 1024 x 1024 pixels. The problems of beam hardening and ring artifacts were removed during post-construction phase. Figure 3.4 shows a typical image of the specimen for the control mix.

3.3 IMAGE PROCESSING

As described before, all images acquired using the HRXCT must be processed before conducting any kind of analysis. The following steps were carried out to process the images to a format that would be suitable for detailed analysis of the microstructure. All steps were carried out using Matlab.

1. Image cropping
2. Contrast enhancement
3. Image noise removal / reduction
4. Thresholding

The two dimensional slice images obtained after scanning were 1024x1024 pixels in size. The images were cropped to a size of 512x512 pixels to obtain the region of interest and remove any unwanted information from the edges. The pixel intensity values of the images obtained in this manner varied from 0 to 165. In order to examine the fine details and visually distinguish between the fine features it is important to fully utilize the entire range of intensity values, i.e. 0 to 255. Therefore a contrast enhancement operation was performed on the cropped images.

All digital images, including the ones used in this study, contain some amount of noise. Eliminating noise while preserving the details of interest in the image is one of the challenges in image

processing. Several different types of linear and nonlinear filtering tools are available to remove different types of noise that is typically present in digital images. Regardless of the type of filter, the output image should minimize noise without destroying the information of interest in the image. The first step to eliminate noise is to identify the type of noise in the image. Multiplicative noise is usually associated with a blur that was not seen in the images. The digital noise in the images was most likely an additive noise. This kind of noise can be reduced by using linear and nonlinear filters. However, linear filters are not the best choice for this study because it is associated with blurring of images and loss of detail at the edges. Figure 2.3 illustrates this for the neighborhood average filter, which is a linear noise filter. Therefore, several different types of non-linear filters were applied to the images (e.g. median filter and anisotropic diffusion). Several images were used with these filters and visually compared. Based on this comparison it was found that the median filter was most effective in reducing noise and preserving details. As described before, in median filtering the gray level of each pixel is replaced by the median of the gray level of all pixel values in the pixel's neighborhood (Russ, 2007). The neighborhood area which is also referred as the kernel, used in this study was 3 by 3. Figure 2.4 demonstrates the use of median filter on a sample image.

A typical mixture composite can be broken down into three components – aggregates, mastic (binder with fines or aggregates finer than 75 microns), and air. After noise reduction the next step was to convert the grayscale image to an image that contained only three pixel intensity values representing the three components within the composite. A thresholding operation was performed such that the end product had air represented by black pixels (pixel value 0), mastic represented by gray (pixel value 150) and aggregate represented by white (pixel value 255). The objective of the thresholding operation is to identify two pixel intensity values in the gray scale image that differentiate between these three components. The volumetric properties (volume of air void and volume of mastic) of each specimen were determined. An iterative process was used to determine the two pixel intensity values that differentiated between air voids, mastic, and the aggregates for a stack of 520 images that represent a volume of the specimen. The iterations were designed to minimize the difference between the volume percent of air voids and mastic computed using the stack of images to the values obtained experimentally. This procedure was based on the work of Zelelew et al. (2008). The thresholds were defined when the computed volume of the mastic and air voids were within a certain tolerance of the known volumes for the mixtures. Since the objective of this study was to characterize the microstructure of the mastic between coarse aggregate particles, a greater emphasis was placed on achieving the correct volume percentage of the mastic. Also, the volume of the specimen that was imaged was a small portion of the specimen that was used to obtain volumetric air content. Therefore, it is possible that the computed values for the air void content from the stack of images may not closely match the air void content of the entire specimen.

For this reason, a broader tolerance was used to compute the threshold for the air void content.

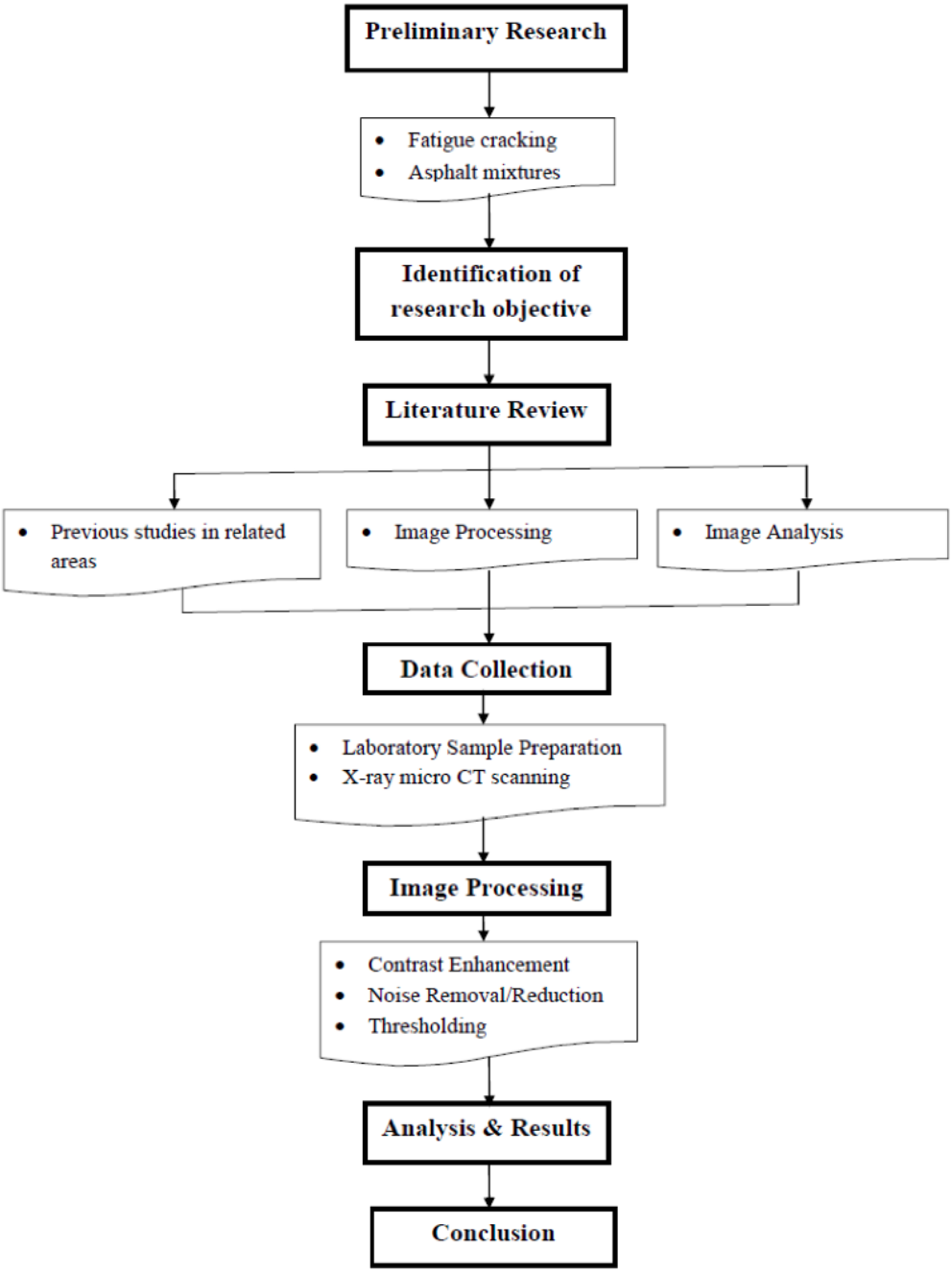

Figure 3.1. Flow Chart of Steps Followed for the Research.

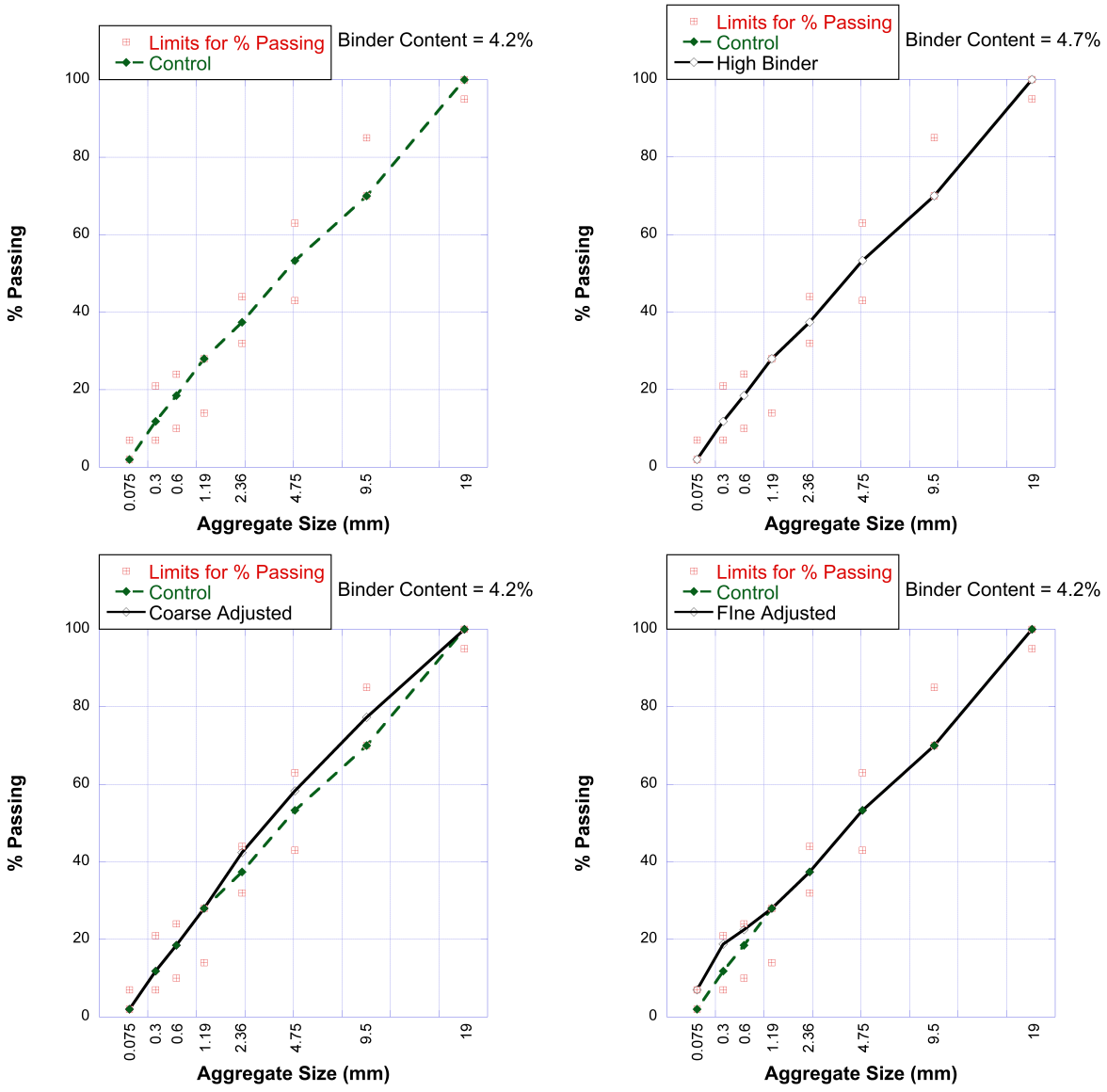

Figure 3.2. Gradations for the Four Different Mixtures.

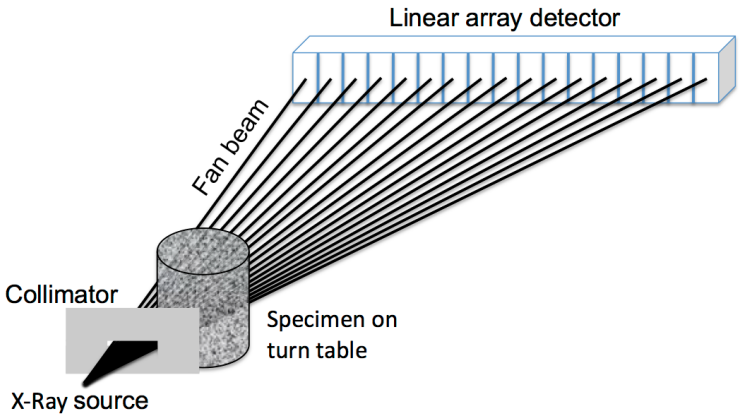

Figure 3.3. Schematic of X-Ray CT Imaging.

(Adapted from Ketcham, 2005a)

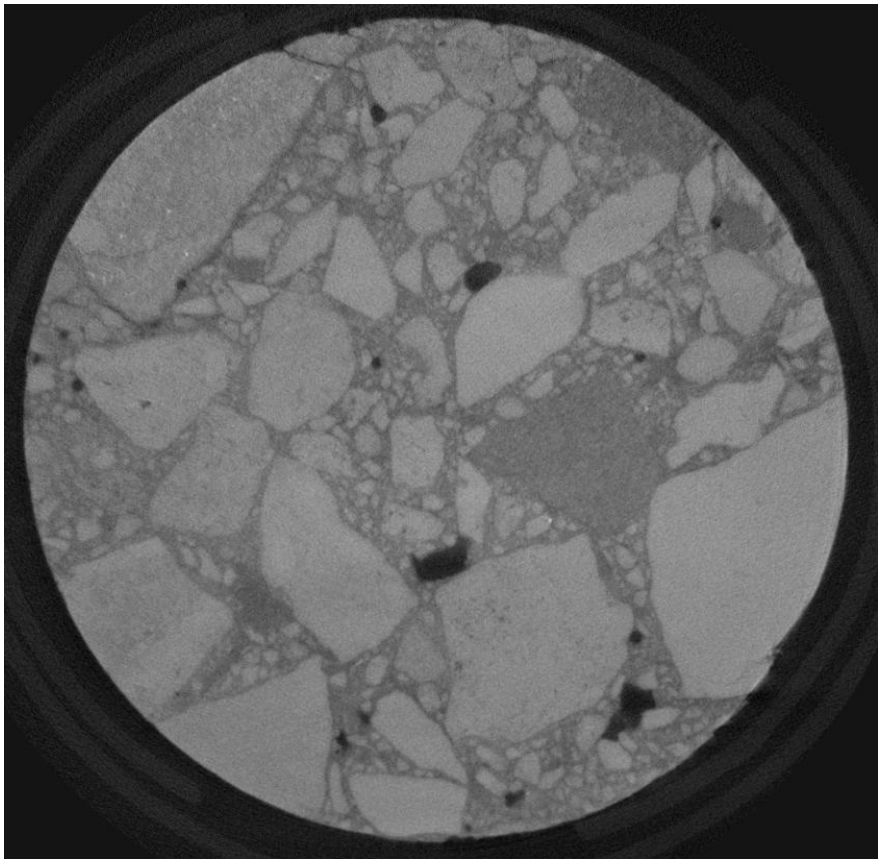

Figure 3.4. Typical HRXRCT Slice Image of Control Mix.

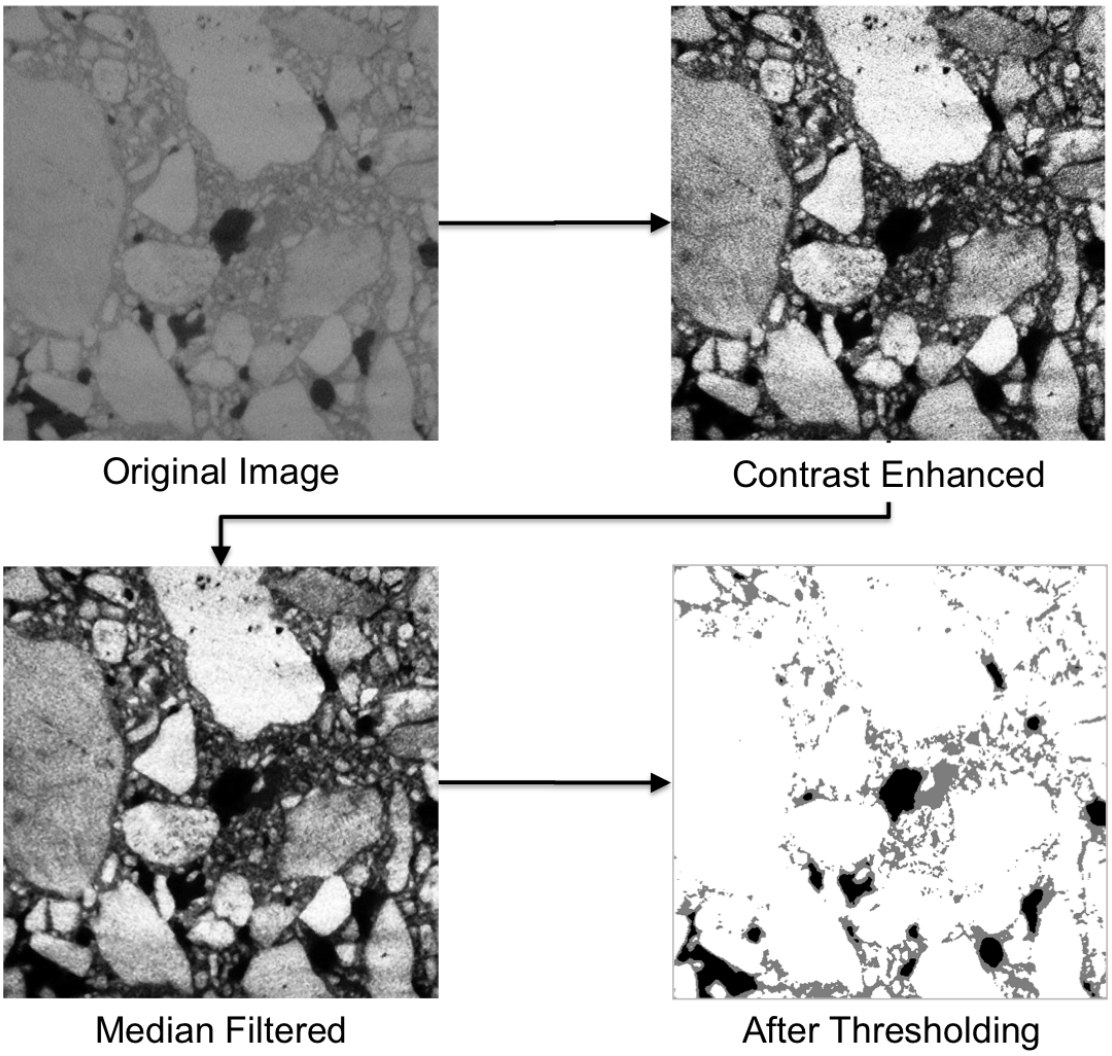

Figure 3.5. Schematic of Image Processing Steps.

CHAPTER 4. ANALYSIS AND RESULTS

4.1 ANALYSIS TO DETERMINE THE MICROSTRUCTURE OF THE ASPHALT MATRIX

The previous chapter summarized the procedures used to fabricate specimens, collect HRXCT image data and process these images to a format that would be suitable for detailed analysis. The main objective of this study is to establish quantitative metrics to characterize the three dimensional microstructure of the asphalt mastic in an asphalt mixture. Based on a literature review, the metric of choice selected for this study was the fabric tensor obtained using the star length distribution (SLD). The Quant3D program originally developed by Ketcham and co-workers was used for analyzing images and characterizing the microstructure of the mastic (2005a). The Quant3D program uses the processed images as an input and computes the SLD (or SVD), fabric tensor, eigen values and eigen vectors for the component of interest. The SLD provides the average length of the component of interest (for specified number of points) along different orientations using a three dimensional rose diagram. For this study, it was also of interest to examine not only the average length but also the distribution of this length along each orientation. Therefore the program was slightly modified to report the distribution of the lengths along each orientation.

Figure 4.1 illustrates the user interface for the Quant3D program. For each specimen 512 processed slice images were uploaded. The critical inputs for this program are as follows. The threshold range of values is used to describe the component of interest. For example, in the processed images, the air voids, mastic, and aggregates are represented using a pixel intensity values of 0, 150, and 255, respectively. For example, in order to analyze the microstructure of the mastic, a range of 145-155 can be used. The "number of directions" defines the number of orientations along which the lengths will be measured. For this study, 512 orientations that represent a uniform distribution on a sphere were selected. A total of 1000 points were randomly selected to make these measurements. Choosing the appropriate number of points is an important parameter to obtain meaningful results. Selection of too many points results in very long computing time. In contrast, selection of too few points will not provide meaningful distributions.

Figures 4.2 and 4.3 illustrate the typical three dimensional rose diagram for the SLD and SVD, respectively. The average SLD is used to compute the fabric tensor using equation 2.4. The eigen vector and eigen values for this fabric tensor are also computed. Recall that the eigen vectors with the largest and smallest eigen values represent the direction vectors along which the moment of inertia is minimized and maximized representing the preferred direction of the matrix. In addition, the ratio of the maximum to the minimum eigen values is a measure of the degree of anisotropy. Table 4.1 lists the fabric tensor, eigenvalues, and eigen vectors based on a typical SLD analysis.

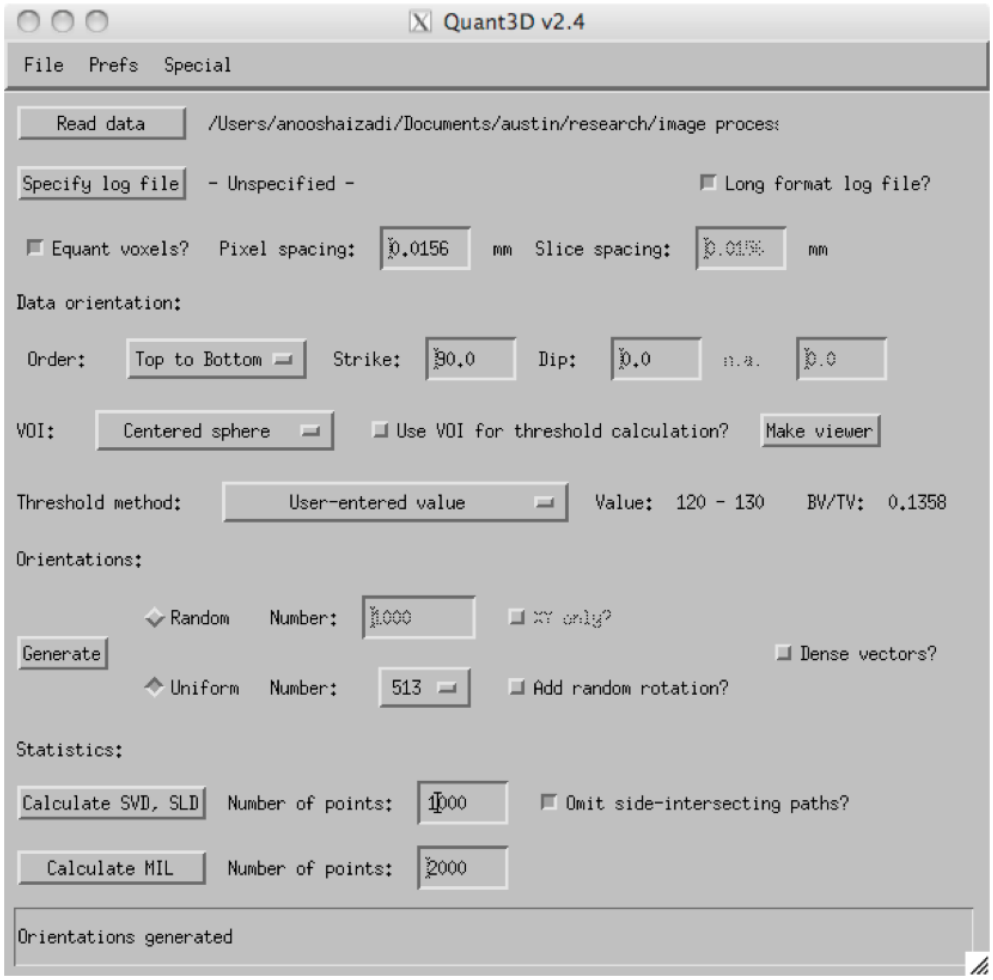

Figure 4.1. Interface for the Quant3D Program.

In summary, the analysis based on SLD provides the following information:

- average three dimensional geometry of the asphalt matrix (in this case the mastic),
- orientation of this geometry with respect to the direction of compaction of the mixture, and
- the degree of anisotropy in the matrix between particles.

Although the above analysis provides the average three dimensional geometry of the matrix between aggregate particles, it does not provide information about the variability in the geometry. The following section describes the methods used to characterize the variability in the microstructure of the asphalt matrix.

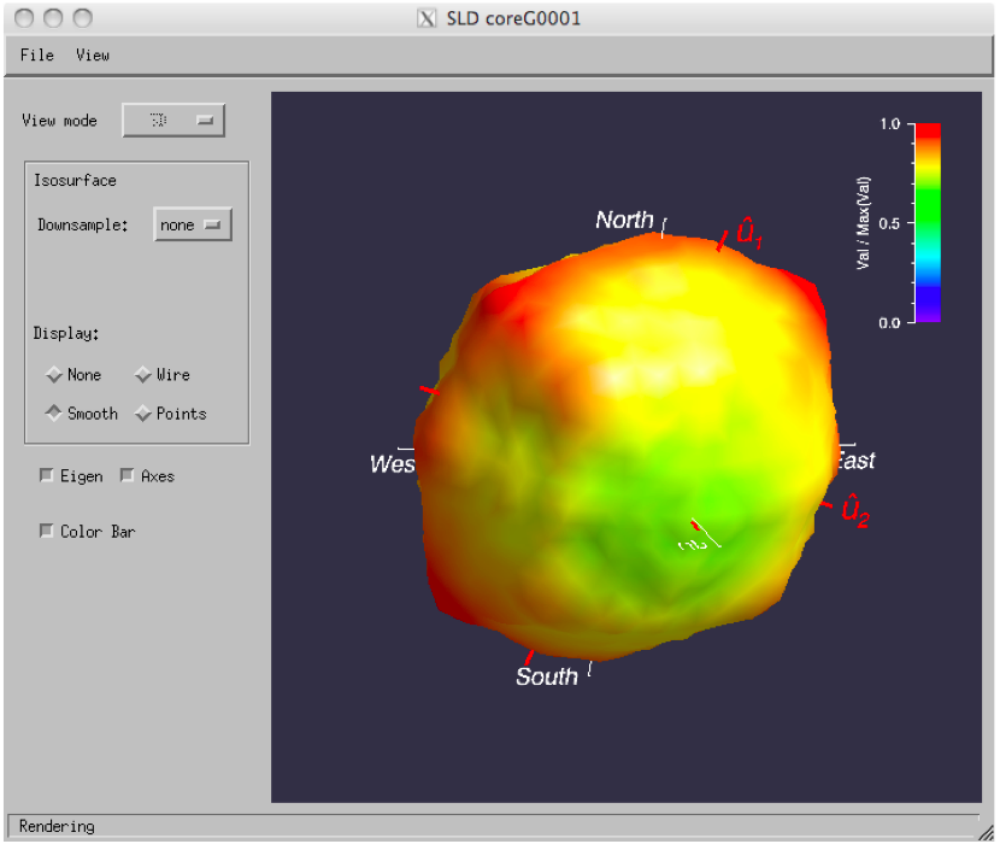

Figure 4.2. Typical Three Dimensional Rose Diagram for SLD from Quant3D.

4.2 VARIABILITY IN THE MICROSTRUCTURE OF THE MATRIX

The Quant3D program was modified to provide star lends at each one of the 1000 points along the 512 directions used in this study. The next was to determine the distribution of the star length along a given direction. A frequency histogram of the star lengths along each direction was plotted. It was found that the Weibull distribution was a reasonably good representation of the distribution of star lengths along each one of the directions. The Weibull distribution has two parameters, shape and scale, that can be varied to fit a wide variety of observed data. The Matlab program was used to obtain the parameters for the Weibull distribution using the 1000 points along each one of the 512 directions. Figure 4.4 illustrates the typical distribution of the star length and the Weibull distribution that was fit using Matlab. The shape and scale parameters for the Weibull distribution were then used to compute the standard deviation and coefficient of variation of the star length along each direction.

The coefficient of variation along different directions were used to plot a three dimensional rose diagram to assess whether or not any particular direction was more susceptible to variability than

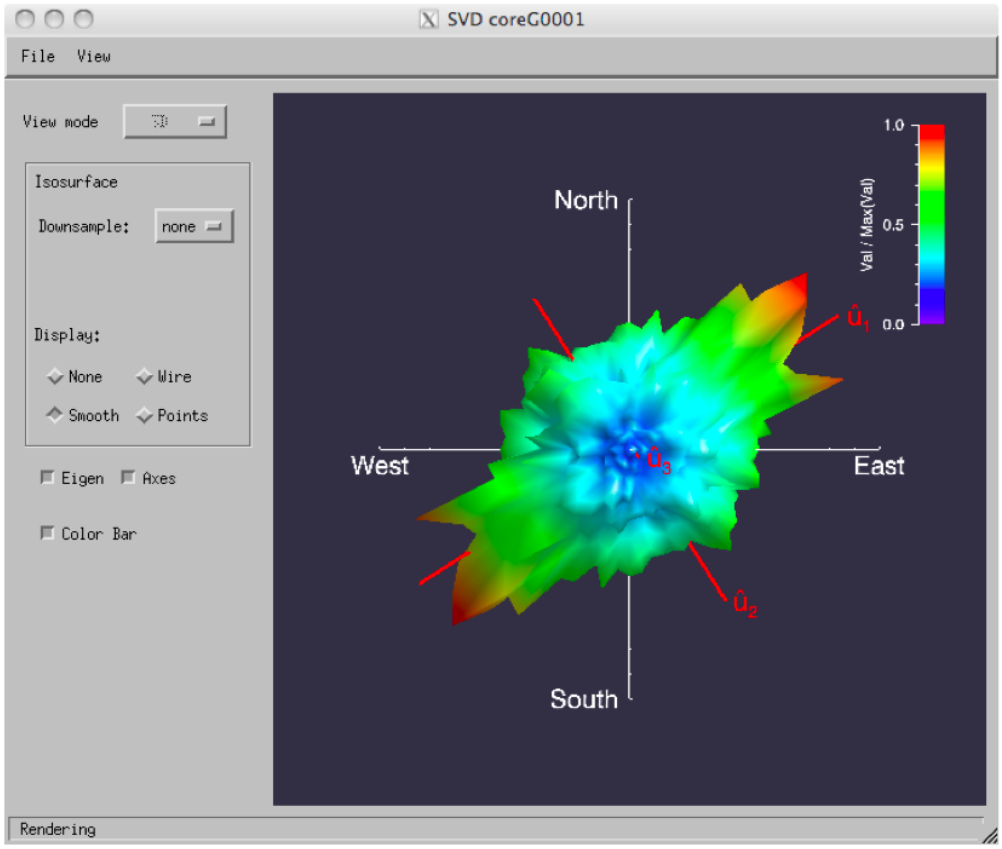

Figure 4.3. Typical Three Dimensional Rose Diagram for SVD from Quant3D.

others (Figure 4.5). This is similar to the rose diagram for the star length distribution, with the difference that the coefficient of variation was used to plot the three dimensional rose diagram. In addition, an average coefficient of variation was also computed for all the 512 directions to be used as a metric to compare the variability of the microstructure between different mixture types.

4.3 RESULTS

The X-ray CT images of two specimens for each of the four mixtures illustrated in Figure 3.2 were processed and analyzed obtain the information described in the aforementioned sections. The microstructure of the matrix for these four mixtures were compared based on the following four metrics:

- Degree of anisotropy: This is defined as the ratio of the maximum to the minimum eigen values.
- Average star length along the preferred direction: The preferred direction is the principal direction that has the highest eigen value. It is also the direction along which the moment of

Table 4.1. Typical Results From Quant3D for SLD Analysis.

Parameter	Value
Fabric Tensor Based on SLD	$\begin{bmatrix} 0.351 & 0.006 & -0.0008 \\ 0.006 & 0.344 & -0.0006 \\ -0.0008 & -0.0006 & 0.3042 \end{bmatrix}$
Eigen vectors	$\begin{bmatrix} 0.8635 & 0.5040 & -0.0191 \end{bmatrix}$
	$\begin{bmatrix} 0.5042 & -0.8636 & 0.0036 \end{bmatrix}$
	$\begin{bmatrix} -0.0147 & -0.0128 & -0.9998 \end{bmatrix}$
Eigenvalues	0.3551
	0.3407
	0.3042
Degree of Anisotropy	1.1672

inertia of the geometry is minimized.

- Average variation in the star lengths along all directions: The analysis was conducted by measuring the star lengths along 513 orientations at 1000 points. The average of the 1000 star lengths along each direction is used to obtain the average three dimensional shape of the matrix. Similarly, the coefficient of variation along each of these 513 directions can be computed for the 1000 points. Since the coefficient of variation along different directions did not vary significantly, the average of the standard deviations and average of the coefficient of variation along the 513 directions were computed and compared for different mixes.

- Orientation or preferred direction of the mastic: This refers to the orientation of the eigen vector with the highest eigen value or lowest moment of inertia. This is also the orientation along which the maximum value of the star length is aligned. The orientation or plunge is the angle made by the vector that defines the preferred direction to the plane perpendicular to the direction of compaction (Figures 4.6 and 4.7).

The results based on the above metrics are summarized in Table 4.2.

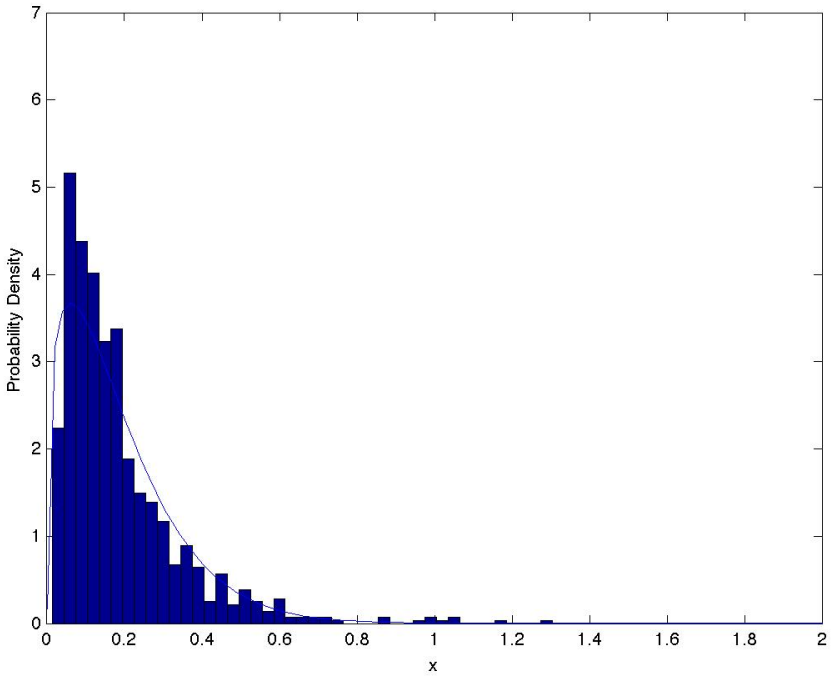

Figure 4.4. Typical Distribution of the Star Length Along a Given Direction.

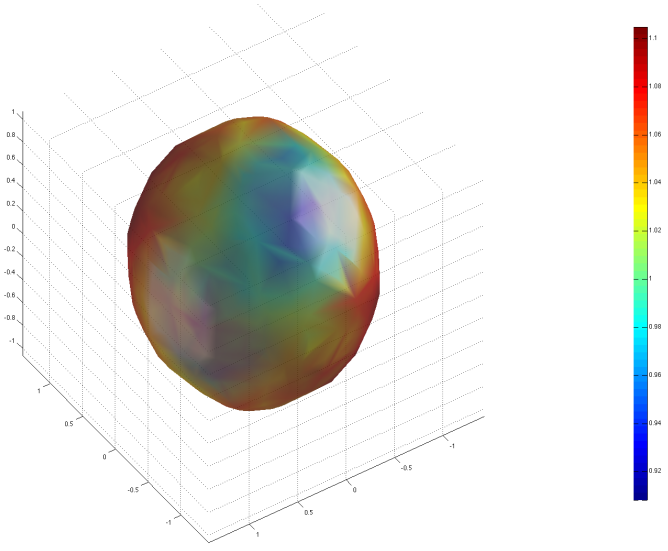

Figure 4.5. Three Dimensional Rose Diagram for the Coefficient of Variation of Star Lengths.

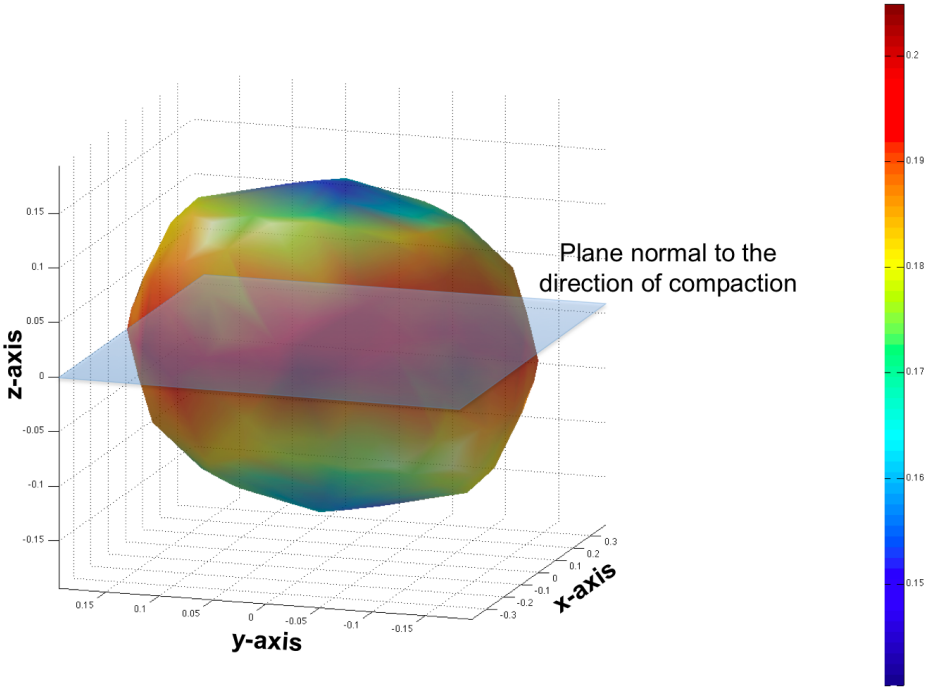

Figure 4.6. Typical Rose Diagram for the SLD with Respect to Axis of Compaction.

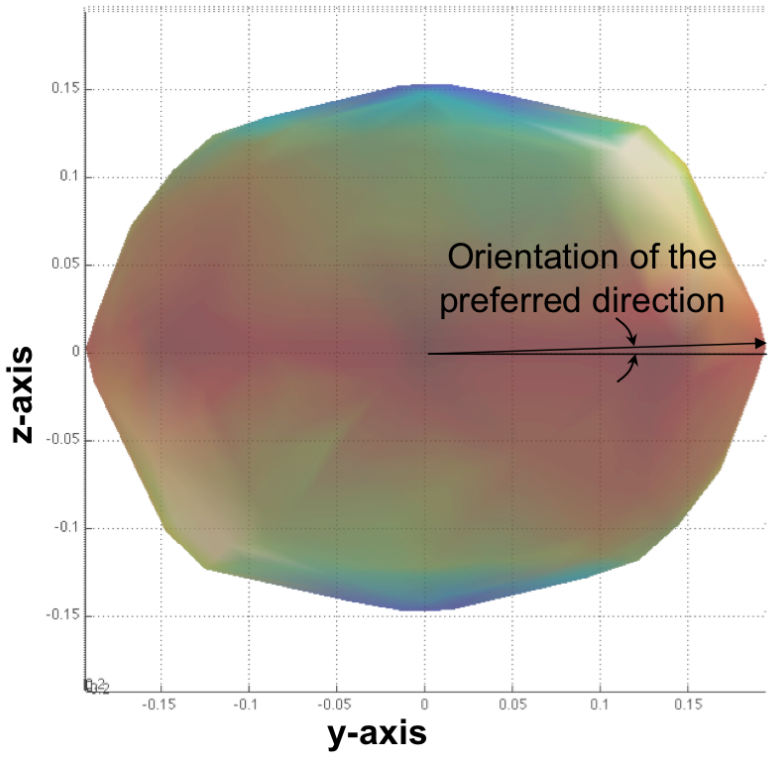

Figure 4.7. Side View Showing Orientation of the Preferred Direction.

Table 4.2. Summary of Results Based on Star Length Analysis of the Matrix.

Mix Type	Degree of anisotropy	Average star length in preferred direction	Average of standard deviation in star lengths	Average of coefficient of variation in star lengths	Orientation of the preferred direction (degrees)
Control Mix	1.28	0.37	0.31	103%	7.6
High Binder	1.25	0.18	0.12	84%	2.8
Fine Adjusted	1.15	0.17	0.13	83%	5.7
Coarse Adjusted	1.30	0.34	0.28	104%	45.4

CHAPTER 5. CONCLUSIONS

The following are some of the conclusions that can be drawn based on the results presented in Table 4.2.

1. The asphalt binder matrix has some degree of anisotropy in all mixtures. The control and the coarse adjusted mixtures had similar and the highest level of anisotropy. This is expected, because the analysis was based on the microstructure of the asphalt matrix which is not expected to change significantly upon changing the only the coarse aggregate gradation of the mixture. Increasing the binder content, reduced the anisotropy to some extent but not significantly. Changing the gradation within the fine aggregate fraction of the mixture significantly reduced the level of anisotropy (fine adjusted mix).

2. The average star length of the asphalt mastic in the fine aggregate matrix along the preferred orientation was similar for the control and the coarse adjusted mix. This was also expected, since changes in the coarse aggregate gradation should not have a significant impact on the internal microstructure of the fine aggregate matrix. The average star length reduced significantly due to the addition of asphalt binder (high binder mix). All other variables remaining constant, contrary to the findings, one would expect that the addition of asphalt binder should increase the average star length as compared to the control mixture. This apparent contradiction can be explained as follows. The fine aggregate particles in mixtures with higher binder content are more likely to be homogeneously distributed resulting in a more dispersed mastic-fine aggregate matrix with relatively smaller average size of the asphalt mastic. This explanation is further supported by the reduced standard deviation and coefficient of variability in the star lengths for the mixtures with higher binder content. A more uniformly dispersed mastic within the matrix can have a significant influence on the mixture properties and performance. For example, a matrix where the asphalt mastic has smaller average dimensions and is more uniformly dispersed can be more effective in crack pinning and hence resisting crack growth. A change in the fine aggregate gradation also had a similar impact as the increase in binder content.

3. In most cases, the preferred direction of the asphalt mastic or direction with the largest star length was perpendicular to the direction of compaction. This indicates that the fine aggregate matrix experiences compaction induced anisotropy in addition to inherent anisotropy that may be due to the shape characteristics of the fine aggregate. For the mixture with the different coarse aggregate gradation (coarse adjusted mix), this orientation was almost 45 degrees to the direction of compaction and significantly different from other mixtures. This

indicates that the coarse aggregate gradation may have an significant influence in dictating the direction of anisotropy.

4. Although all test specimens had gradations within the specification limits, they had widely different internal microstructure. The differences in the internal microstructure are expected to yield very different mechanical and damage characteristics. While the findings reported in this study are based on the use of a limited number of mixtures, the results indicate the importance of understanding the relationship between aggregate gradation, internal microstructure, and performance.

REFERENCES

Arambula, E., Masad, E., and Martin, A. E. 2007. Influence of air void distribution on the moisture susceptibility of asphalt mixes. *Journal of Materials in Civil Engineering*, 19(8):655–664.

Cowin, S. C. 1985. The relationship between the elasticity tensor and the fabric tensor. *Mechanics of Materials*, 4(2):137 – 147.

Duxson, P., Provis, J. L., Lukey, G. C., Mallicoat, S. W., Kriven, W. M., and van Deventer, J. S. 2005. Understanding the relationship between geopolymer composition, microstructure and mechanical properties. *Colloids and Surfaces A: Physicochemical and Engineering Aspects*, 269(1-3):47 – 58.

Elseifi, M., Al-Qadi, I., Yang, S., and Carpenter, S. 2008. Validity of asphalt binder film thickness concept in Hot-Mix asphalt. *Transportation Research Record: Journal of the Transportation Research Board*, 2057:37–45.

Harrigan, T. P. and Mann, R. W. 1984. Characterization of microstructural anitsotropy in orthotropic materials using a second rank tensor. *Journal of Materials Science*, 19:761–767.

Hunter, A., Airey, G., and Collop, A. 2004. Aggregate orientation and segregation in Laboratory-Compacted asphalt samples. *Transportation Research Record: Journal of the Transportation Research Board*, 1891:8–15.

Ketcham, R. A. 2005a. Computational methods for quantitative analysis of three-dimensional features in geological specimens. *Geosphere*, 1(1):32–41.

Ketcham, R. A. 2005b. Three-dimensional grain fabric measurements using High-Resolution X-Ray computed tomography. *Journal of Structural Geology*, 27:1217–1228.

Ketcham, R. A. and Carlson, W. D. 2001. Acquisition, optimization and interpretation of x-ray computed tomographic imagery: Applications to the geosciences. *Computers & Geosciences*, 27(4):381–400.

Masad, E. and Button, J. 2004. Implications of experimental measurements and analyses of the internal structure of Hot-Mix asphalt. *Transportation Research Record: Journal of the Transportation Research Board*, 1891:212–220.

Masad, E., Muhunthan, B., Shashidhar, N., and Harman, T. 1999a. Internal structure characterization of asphalt concrete using image analysis. *Journal of Computing in Civil Engineering*, 13(2):88–95.

Masad, E., Muhunthan, B., Shashidhar, N., and Harman, T. 1999b. Quantifying laboratory compaction effects on the internal structure of asphalt concrete. *Transportation Research Record: Journal of the Transportation Research Board*, 1681:179–185.

Masad, E., Tashman, L., Somedavan, N., and Little, D. 2002. Micromechanics-Based analysis of stiffness anisotropy in asphalt mixtures. *Journal of Materials in Civil Engineering*, 14(5):374–383.

Odgaard, A. 1997. Three-dimensional methods for quantification of cancellous bone architecture. *Bone*, 20(4):315 – 328.

Russ, J. 2007. *The image processing handbook*. CRC/Taylor and Francis, Boca Raton, 5th ed. edition.

Ryan, T. M. and Ketcham, R. A. 2002. The three-dimensional structure of trabecular bone in the femoral head of strepsirrhine primates. *Journal of Human Evolution*, 43(1):1 – 26.

Tashman, L., Masad, E., Little, D., and Zbib, H. 2005. A microstructure-based viscoplastic model for asphalt concrete. *International Journal of Plasticity*, 21(9):1659–1685.

Torquoato, S. and Lu, B. 1993. Chord-length distribution function for two-phase ramdom media. *Physical Review E*, 47(4):2950–2954.

Tutumluer, E., Huang, H., Hashash, Y. M. A., and Ghaboussi, J. 2008. Imaging based discrete element modeling of granular assemblies. *AIP Conference Proceedings*, 973(1):544–549.

Wang, L., Frost, J., and Shashidhar, N. 2001. Microstructure study of WesTrack mixes from X-Ray tomography images. *Transportation Research Record: Journal of the Transportation Research Board*, 1767(-1):85–94.

Wang, L., Park, J., and Fu, Y. 2007. Representation of real particles for DEM simulation using x-ray tomography. *Construction and Building Materials*, 21(2):338–346.

Watson, G. S. 1966. The statistics of orientation data. *The Journal of Geology*, 74(5):786–797.

You, Z., Adhikari, S., and Kutay, M. E. 2009. Dynamic modulus simulation of the asphalt concrete using the x-ray computed tomography images. *Materials and Structures*, 42(5):617–630.

Yue, Z. Q., Bekking, W., and Morin, I. 1995. Application of digital image processing to quantitative study of asphalt concrete microstructure. *Transportation Research Record*, 1492:53–60.

Zelelew, H., Papagiannakis, A. T., and Masad, E. 2008. Application of digital image processing techniques for asphalt concrete mixture images. In *The 12th International Conference of IACMAG*, pages 119–124, Goa, India.